Title
Spontaneous Chelation-Driven Reduction of the Neptunyl Cation in Aqueous Solution.

Journal
Chemistry (Weinheim an der Bergstrasse, Germany), 26(11)

ISSN
0947-6539

Authors
Carter, Korey P
Smith, Kurt F
Tratnjek, Toni
et al.

Publication Date
2020-02-01

DOI
10.1002/chem.201905695

Peer reviewed

Spontaneous Chelation-Driven Reduction of the Neptunyl Cation in Aqueous Solution

Korey P. Carter,[a] Kurt F. Smith,[a] Toni Tratnjek,[a] Katherine M. Shield,[a, b] Liane M. Moreau,[a] Julian A. Rees,[a] Corwin H. Booth,*[a] and Rebecca J. Abergel*[a, b]

Abstract: Octadentate hydroxypyridinone (HOPO) and catecholamide (CAM) siderophore analogues are known to be efficacious chelators of the actinide cations, and these ligands are also capable of facilitating both activation and reduction of actinyl species. Utilizing X-ray absorption near edge structure (XANES) and extended X-ray absorption fine structure (EXAFS) spectroscopies, as well as cyclic voltammetry measurements, herein, we elucidate chelation-based mechanisms for driving reactivity and initiating redox processes in a family of neptunyl–HOPO and CAM complexes. Based on the selected chelator, the ability to control the oxidation state of neptunium and the speed of reduction and concurrent oxo group activation was demonstrated. Most notably, reduction kinetics for the $Np^{V}O_2^{+/}Np^{IV}$ redox couple upon chelation by the ligands 3,4,3-LI(1,2-HOPO) and 3,4,3-LI$(CAM)_2$(1,2-$HOPO)_2$ was observed to be faster than ever reported, and in fact quicker than we could measure using either X-ray absorption spectroscopy or electrochemical techniques.

Neptunium (Np) was first experimentally isolated by McMillan and Abelson in 1940 at the Berkeley Radiation Laboratory[1] and features chemical properties similar to its better-known neighbors uranium (U) and plutonium (Pu).[2] Knowledge of Np chemistry is particularly important for nuclear-waste storage and processing as ^{237}Np, in the form of the NpO_2^+ cation, is found in considerable quantities in high-level nuclear waste and is highly water soluble, yet the chemistry of Np has been largely neglected compared to U and Pu.[3] The significant mobility of Np in the environment also introduces risks for radiological contamination, which is a current topic of critical concern.[4] Once internalized in the human body, Np ions move rapidly throughout the bloodstream and are primarily deposited in the liver and bones.[5] Clearance following uptake and deposition of Np is slow, and similar to other actinide cations, Np presents severe health risks due to its chemical and radiological toxicity.[4b] Decorporation by metal-ion chelation is considered the best method for promoting excretion of actinides in vivo; however, no effective chelator for Np decorporation is currently approved by the U.S. Food and Drug Administration.[6]

Multidentate hydroxypyridinone (HOPO) and catecholamide (CAM) ligands are known to have a peerless affinity for actinide cations.[7] HOPO chelators, in particular, are also known to chelate both actinide (An) and lanthanide (Ln) cations exceptionally well both in vitro and in vivo, and have been shown to be effective decorporation agents in multiple animal models.[6,8] In fact, the octadentate 3,4,3-LI(1,2-HOPO) (Scheme 1), denoted 343-HOPO hereafter, was shown to be capable of increasing not only Pu^{IV} and Am^{III} excretion in vivo, but that of actinyl species, that is, U^{VI} and Np^{V}, as well, in stark contrast to DTPA.[8b] The mechanism for the latter findings is not well understood as solution thermodynamics measurements highlight significant differences in the affinity of 343-HOPO for M^{IV} and M^{III} actinides in comparison to actinyl cations.[9] Reduction of Np^{V} to Np^{IV} is possible, with chelation-driven reduction to Np^{IV} predicted to be an efficient decorporation pathway for Np^{V}.[8a]

Complexation-induced Np reduction, from $+5$ to $+4$, has been observed both synthetically and in the environment,[10] yet the electron-transfer kinetics of Np–oxo bond cleavage are known to be extremely slow.[3b] This makes the Np^{V}/Np^{IV} redox couple hard to evaluate[3c] and has thus far limited the applicability of chelation-driven reduction as a means for Np decorporation. Recently, we observed chelation-driven activation and concurrent reduction of neptunyl and plutonyl cations in the gas phase along with complexation-induced Np reduction in the condensed phase, yet were not able to definitively capture and identify the reduced species in solution.[11] Herein, we follow up on this initial chelation-driven Np^{V} activation and reduction work with the first systematic study of Np chelates featuring 343-HOPO, as well as three synthetic analogues. The additional 343 ligands are also built on the spermine backbone and incorporate either four CAM metal-binding groups, 3,4,3-LI(CAM) (Scheme 1), denoted 343-CAM hereafter, or a combination of HOPO and CAM moieties directed by selective attachment to the primary or secondary amines of the scaffold, 3,4,3-LI$(CAM)_2$(1,2-$HOPO)_2$ and 3,4,3-LI(1,2-$HOPO)_2(CAM)_2$, respective-

[a] *Dr. K. P. Carter, Dr. K. F. Smith, T. Tratnjek, K. M. Shield, Dr. L. M. Moreau, Dr. J. A. Rees, Dr. C. H. Booth, Prof. Dr. R. J. Abergel*
Chemical Sciences Division
Lawrence Berkeley National Laboratory, Berkeley, CA 94720 (USA)
E-mail: chbooth@lbl.gov
abergel@berkeley.edu

[b] *K. M. Shield, Prof. Dr. R. J. Abergel*
Department of Nuclear Engineering, University of California
Berkeley, CA 94709 (USA)

Supporting information and the ORCID identification number(s) for the author(s) of this article can be found under: https://doi.org/10.1002/chem.201905695. It contains experimental details, additional figures and tables from XANES and EXAFS spectra, as well as additional CV spectra.

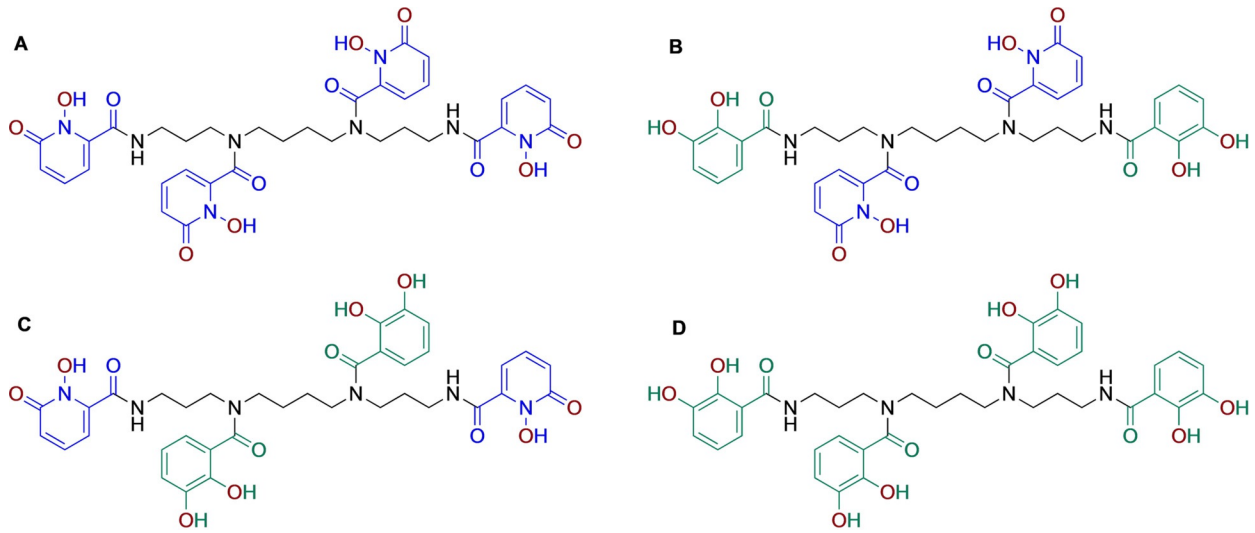

Scheme 1. Spermine-based octadentate ligands. For each ligand, the 3,4,3-LI scaffold is connected through amide linkages to four metal-binding units, which are either 1,2-HOPO (blue) or CAM (green) moieties (metal-binding atoms highlighted in red). Only four ligand combinations are easily accessible through classical synthetic methods: A) 3,4,3-LI(1,2-HOPO); B) 3,4,3-LI(CAM)$_2$(1,2-HOPO)$_2$; C) 3,4,3-LI(1,2-HOPO)$_2$(CAM)$_2$; and D) 3,4,3-LI(CAM) (respectively denoted 343-HOPO, 343-CHHC, 343-HCCH, and 343-CAM hereafter).

ly abbreviated 343-CHHC and 343-HCCH (Scheme 1).[12] Utilizing X-ray absorption near edge structure (XANES) and extended X-ray absorption fine structure (EXAFS) spectroscopies, as well as cyclic voltammetry measurements, we demonstrate the ability to control the oxidation state of Np based on the selected chelator. With 343-HOPO and 343-CHHC, we observe nearly instantaneous reduction of Np^{V} to Np^{IV}, whereas 343-HCCH also results in Np reduction but the process is much slower at neutral pH (days rather than seconds). Finally, with 343-CAM, no reduction is observed, and Np remains as the NpO_2^+ species in solution. The nearly instantaneous reduction of Np^{V} by 343-HOPO and 343-CHHC, with kinetics too fast to measure via X-ray absorption or electrochemical techniques, is the first example of efficient cleavage of Np-oxo bonds in solution, and these results explain the extraordinary in vivo Np decorporation ability of 343-HOPO observed previously.[8b]

A series of aqueous samples of Np^{V} with each of the 343 ligands were prepared at pH 7–8 to ensure ligand deprotonation and formation of a single species in solution. Samples were triply contained in aluminum sample holders, and XANES and EXAFS spectra were measured at 50 K in fluorescence mode on beamline 11-2 at the Stanford Synchrotron Radiation Lightsource (SSRL). The high photon flux and 100-element Ge detector available at SSRL facilitated data collection at the Np L_{III}-edge using only 59.3 μg of ^{237}Np per sample (see the Supporting Information for details).

XANES spectroscopy can be used to determine metal oxidation states in solution, which is generally done by comparing spectral characteristics, such as edge energy to known standards for a given element.[13] XANES spectra at the Np L_{III}-edge of all four Np-343 ligand complexes are shown in Figure 1, and these results highlight the challenge in using XANES to determine Np oxidation states. The samples were checked for beam-induced redox changes by monitoring white-line intensity as a function of time (Figure 1 and the Supporting Information), and this demonstrated that all samples were stable under the beam with the exception of Np-343-HOPO in which a small (< 5 %) change in white-line intensity throughout the measurement was observed. Previous work has highlighted that the Np white line and inflection point energies are not directly correlated with increasing oxidation state as the change in local structure from Np^{x+} to NpO_2^{y+} (in which $x = 3$ or 4 and $y = 1$ or 2) also influences the ionization energy of the absorb-

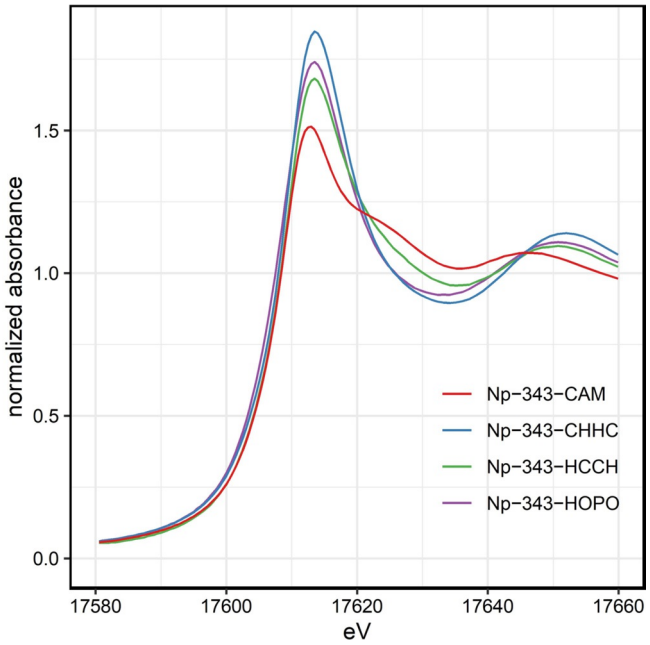

Figure 1. Comparison of Np L_{III}-edge XANES spectra for aqueous Np-343 ligand complexes at 50 K. The presence of an 'yl' shoulder at approximately 17625 eV in the Np-343-HCCH and Np-343-CAM XANES spectra suggests the possibility of a mixed valence state for Np-343-HCCH and that Np-343-CAM predominantly features Np as the neptunyl cation ($Np^{V}O_2^+$).

ing atom.[14] There is still a pathway for distinguishing Np oxidation states; however, stemming from the multiple scattering resonance at the high-energy flank of the white line of a Np^{V} sample. This feature stems from scattering along the axial oxygen atoms of the linear neptunyl moiety and is described as an 'yl' shoulder. Clearly discernible 'yl' shoulders can be seen in the spectra of Np-343-HCCH and Np-343-CAM between 17620 and 17630 eV (Figure 1), with the position determined by the amount of Np^{V} in solution and the actual Np–oxo bond lengths in these two complexes. The lack of 'yl' shoulders in the XANES spectra for Np-343-HOPO and Np-343-CHHC are indicative of complete reduction of Np^{V} to Np^{IV}, whereas the partial shoulder in the spectra of Np-343-HCCH hints at a possible mixed valent Np^{V}/Np^{IV} species. Finally, the clear 'yl' shoulder in the XANES spectra for Np-343-CAM is suggestive that little or no reduction occurred, which means the $Np^{V}O_2^{+}$ moiety likely predominates. To confirm these oxidation state assignments, we turned to local structure comparisons from EXAFS spectroscopy at the Np L_{III}-edge on all four complexes.

EXAFS spectroscopy was employed to acquire information about the local structure arrangement around Np cations, and high-quality data were obtained from 2.5–10 $Å^{-1}$ (in k space). Figure 2 shows the Fourier transforms (FTs) and corresponding k^3-weighted Np L_{III}-edge EXAFS spectra, with all fitting statistics included in Table S1 (in the Supporting Information). Qualitatively, most of the EXAFS signals are well described by a fitting model based on calculated An-HOPO structures,[15] and for each dataset, the bond lengths (R) and Debye–Waller factors (σ^2) were determined.

The fitting models for Np-343-HOPO and Np-343-CHHC complexes (Figure 2) assume the first scattering shell is attributed to a single shell of eight O scatterers, and both models also include a second shell that comprises a full complement of 4 C and 4 N neighbors at approximately 3.28 Å. This is broadly consistent with expectations for HOPO and CAM ligands, and Np–O bond lengths with 343-HOPO and 343-CHHC are approximately 2.39 Å, which is in excellent agreement with M^{IV}–O distances predicted by DFT calculations for Np.[15] The FT of the EXAFS spectra for Np-343-CAM revealed the characteristic two peaks that are known for actinyl moieties (Figure 2). As a result, we included two oxygen scatterers at 1.84 Å in the first shell of the Np-343-CAM fit, and this gave a very reasonable

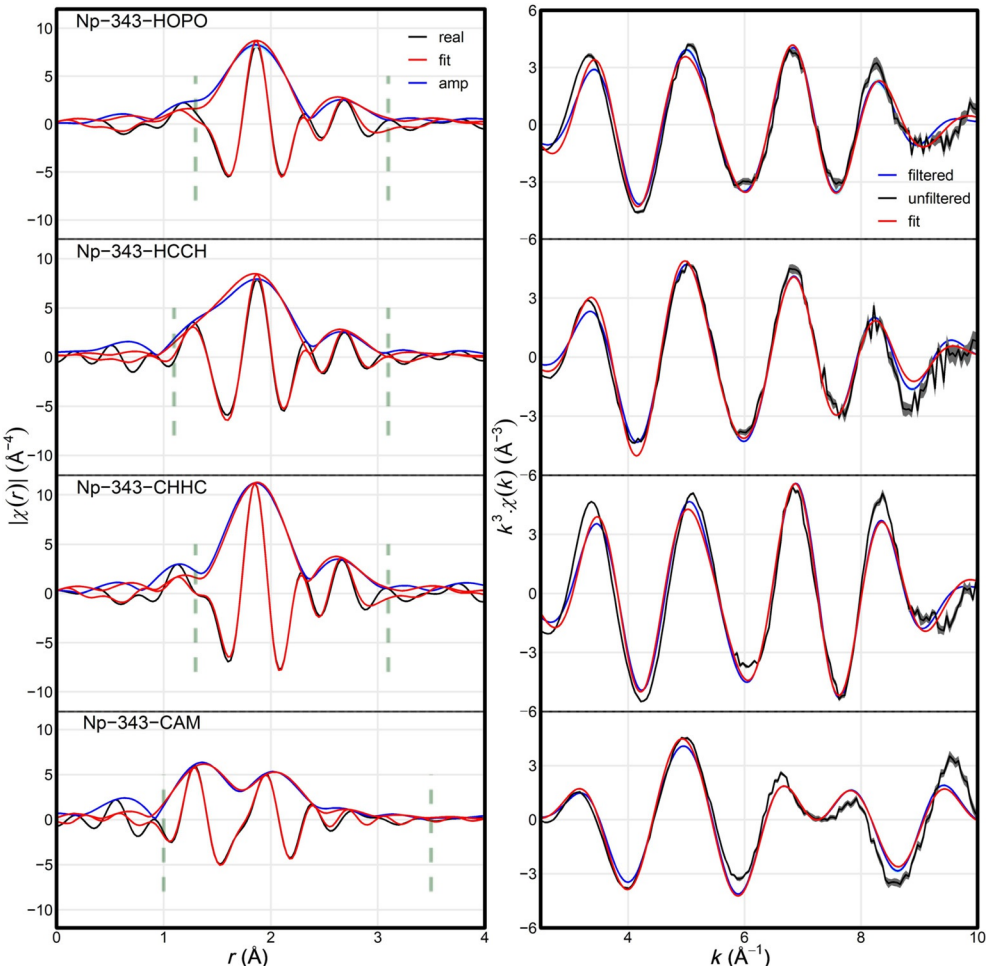

Figure 2. EXAFS data and fit results for aqueous Np-343 ligand complexes at 50 K. Left: Fourier transforms (FT) of the k-space data and fit. Vertical dashed lines indicate the fit range. Data were transformed between 2.5 and 10 $Å^{-1}$ by using a Gaussian window with a width of 0.3 $Å^{-1}$. The raw unfiltered data error bars (encompassed by the solid gray shaded area around the data set) were estimated by the standard deviation of the mean between traces. Right: EXAFS results in k-space. The filtered data and fit were back-transformed over the fit range (see the Supporting Information for details).

Debye–Waller factor of 0.004 Å^2.[14b] The successful modeling of two short Np–oxo moieties confirms the presence of NpO_2^+, and the second shell of the Np-343-CAM fit included four oxygen scatterers at 2.49(1) Å and four carbon scatterers at approximately 3.4 Å.

The EXAFS spectra for the Np-343-HCCH complex is more interesting, because it could not be satisfactorily fit as only a Np^{IV} species due to a substantial shoulder in the FT at low *R* that is unaccounted for in the first shell (Figure 2). XANES spectra for Np-343-HCCH (Figure 1) did reveal an 'yl' shoulder suggesting the presence of some amount of Np^V, and when the fit for the Np-343-HCCH complex is updated to account for a contribution from the short axial oxygens associated with the neptunyl moiety, fit metrics improve significantly. To confirm the presence of Np^V, an F test was conducted on the inclusion of axial O atoms in the fit (Table S2 in the Supporting Information). A pair of axial O scatterers at approximately 1.85 Å (in contrast to ca. 2.5 Å for O scatterers in the equatorial plane) would be diagnostic of a pure Np^V sample. The inclusion of a single O scatterer (ca. 50% Np^V) at 1.85 Å passed an F test with 99% confidence indicating Np^V was making a contribution to the EXAFS of the Np-343-HCCH complex. To provide a more robust quantification of the Np^V contribution to the Np-343-HCCH dataset, a final fit was conducted where the Debye–Waller factor for the neptunyl moiety was set to a reasonable value of 0.0025 Å^2.[14b] This fit gave a value of 0.8 Np–oxo scatterers in the first shell, implying approximately 40% of Np present in Np-343-HCCH is in the +5 oxidation state, which means the Np-343-HCCH complex is a mixed valent Np^V/Np^{IV} species.

To determine the electrochemical stability of the free ligands and the Np-343 ligand complexes in aqueous media, cyclic voltammetry (CV) measurements were carried out over the potential range −200 to 1000 mV (vs. Ag/AgCl electrode) at a sweep rate (υ) of 50 mV s^{-1}. Voltammograms of the free 343-HOPO and the 343-mixed ligand chelators are shown in Figures S2 and S3 (in the Supporting Information), respectively. A non-reversible oxidation of 343-HOPO is observed at an anodic potential (E_a) of 790(10) mV, which is attributed to the oxidation of an oxygen atom on one of the 1,2-HOPO moieties. The absence of a reduction peak indicates either that the reaction was not reversible or that the oxidation product quickly underwent a subsequent reaction. Similar behavior was observed with the ligand 343-CHHC, with the presence of two oxidation waves located at E_a = 505(6) and 835(10) mV. The wave at higher potential is assigned as an oxidation of a 1,2-HOPO functional group (see above), while the wave at lower potential correlates with redox couple values reported for simple catecholamines.[16] 343-HCCH presented a weak oxidation wave at E_a = 830(12) mV, corresponding to the oxidation of one 1,2-HOPO moiety, as depicted in Figure S3 (in the Supporting Information).

The voltammograms of Np-343-complexes (with 343-HOPO, 343-CHHC, and 343-HCCH) presented in Figure 3 show almost no signs of oxidation or reduction of the metal center during the experiments. Generally, the slow electron-transfer kinetics of the Np^V/Np^{IV} couple make it hard to probe via cyclic voltammetry;[3c] however, we had the opposite problem as the immediate color change of the solution inside the CV cell for all three samples, including 343-HCCH, indicated a reduction event was taking place faster than we could obtain CV data. Additionally, we did not observe redox potentials at either approximately 900 mV, which would have been expected for the Np^{VI}/Np^V couple,[17] or below −150 mV, which is where the Np^{IV}/Np^{III} couple is located.[3c,17a] These results are largely consistent with the XAS results (see above), and we attribute the complete reduction of Np^V by 343-HCCH to the lower pH of CV experiments (ca. 4.5) compared to EXAFS measurements (ca. 7). Interestingly, we do see a small oxidation peak at approximately 200(10) mV in the voltammogram of Np-343-CHHC, and while this peak is not due to the CAM or 1,2-HOPO functional groups we hesitate to assign this as a metal-based event in the absence of more rigorous experimental and theo-

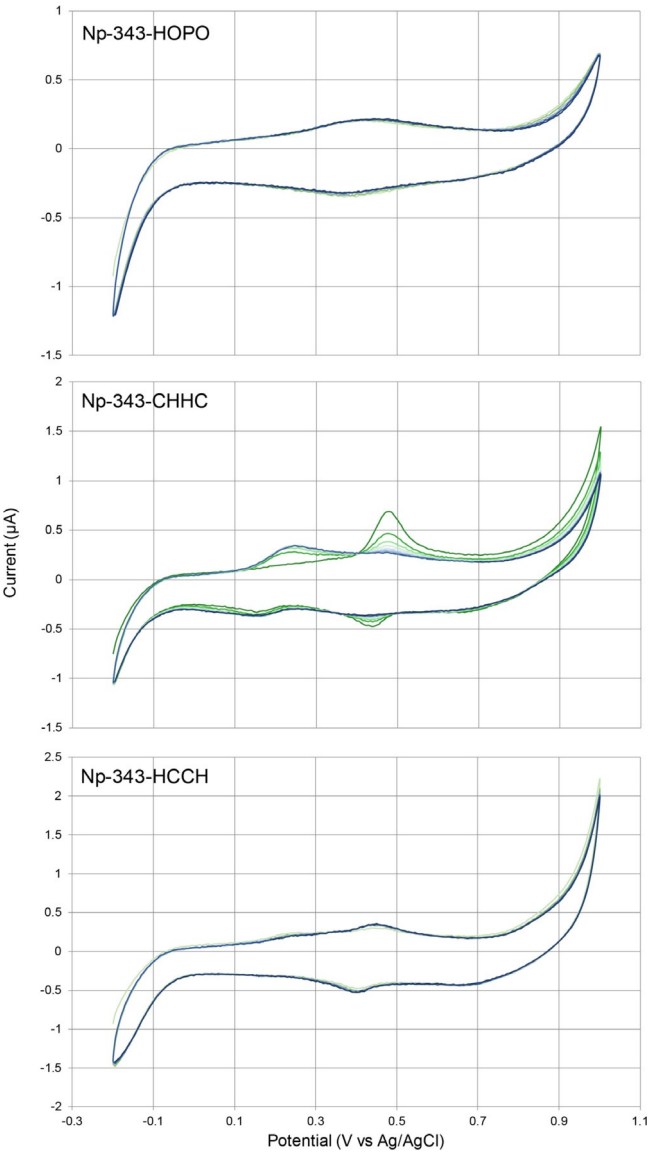

Figure 3. Cyclic voltammograms of 0.5 mM Np complexes of 343-HOPO (top), 343-CHHC (middle), and 343-HCCH (bottom) in 1 M SO_4^{2-} buffered to pH 4.5 with sodium acetate.

retical characterization. When bound to Np, the CAM moieties in both 343-CHHC and 343-HCCH appear to remain weakly active. 343-CHHC has an anodic potential E_a observed at 480(5) mV and a cathodic potential (E_c) observed at 430(10) mV, whereas with 343-HCCH (Figure 3), an enhancement of the activity was observed with $E_a = 460(5)$ and $E_c = 400(5)$ mV, leading to potential differences (ΔE_p) of approximately 50 and 60 mV, respectively, indicative of Nernstian systems.

Comparing the fate of Np-343-HOPO and Np-343-CAM complexes, it appears that the deprotonated 1,2-HOPO binding moiety is the key driver for the Np^V reduction and oxo bond cleavage. This finding is in line with those from De Proft et al. who showed that the most efficient redox non-innocent ligands with a X=C–C=Y structural motif use electronegative contact atoms (N, O, or S for X and Y) tethered with a delocalized chain to avoid unstable localized radicals upon reduction.[18] In fact, the high acidity of the pyridinium proton in 1,2-HOPO functional groups (compared with the hydroxyl protons in CAM moieties) is due to the delocalization by aromatic resonance of the nitrogen pair of electrons. However, one particularly interesting result of this study is the significantly faster neptunyl reductive activation rate achieved by 343-CHHC compared with 343-HCCH under the neutral solution conditions maintained for XAS measurements. A notable difference between the two ligands is the positioning of the 1,2-HOPO or CAM amide linkers on the spermine internal/secondary or external/primary amine groups. We hypothesize that the remaining proton on the external amide nitrogen can readily form hydrogen bonds with the deprotonated, metal-bound hydroxyl oxygen in 343-HCCH, thereby diminishing the electron-donating character of the metal-binding group, which is likely central to the Np reduction process. 343-HCCH is capable of completely reducing Np^V to Np^{IV}, yet this required the lower pH values (ca. 4.5) used during CV measurements. This phenomenon could be explained by the protonation of the more basic hydroxyl oxygens at the *meta* position of the CAM moieties at lower pH values, resulting in stronger electron-withdrawing character on the metal ion, which would in turn become more prone to reduction from the 1,2-HOPO functional groups.

In summary, spontaneous chelation-driven reduction of the NpO_2^+ moiety was observed in the condensed phase. XANES and EXAFS spectroscopy on Np-343 ligand complexes confirmed metal-ion reduction, providing some of the first structural data on a mixed valent Np^V/Np^{IV} chelate, while also rationalizing previously observed Np-343-HOPO decorporation results. The kinetics of Np^V reduction were too fast to measure by either X-ray absorption or electrochemical techniques, representing a significant advance in Np coordination chemistry as Np^V/Np^{IV} redox chemistry has previously been hindered by sluggish electron-transfer processes. Since An^V/An^{IV} interactions are of significant importance in the nuclear reprocessing and actinide-migration schemes,[19] work is in progress to better understand the mechanism of Np reduction via UV/Vis spectroelectrochemistry, with future aims to extend the chemistry highlighted herein to plutonium and americium systems.

Acknowledgements

We thank Dr. Gauthier Deblonde for helpful discussions and Dr. Wayne Lukens for providing the ^{237}Np starting material. This work was supported by the U.S. Department of Energy (DOE), Office of Science, Office of Basic Energy Sciences, Chemical Sciences, Geosciences, and Biosciences Division at the Lawrence Berkeley National Laboratory under Contract DE-AC02-05CH1123. K.M.S. acknowledges support from a U.S. DOE Integrated University Program graduate research fellowship. Use of the Stanford Synchrotron Radiation Lightsource, SLAC National Accelerator Laboratory, is supported by the U.S. DOE, Office of Science, Office of Basic Energy Sciences under Contract No. DE-AC02-76SF00515.

Conflict of interest

The authors declare no conflict of interest.

[1] E. McMillan, P. H. Abelson, *Phys. Rev.* **1940**, *57*, 1185 – 1186.

[2] a) G. R. Choppin, *Radiochim. Acta* **1983**, *32*, 43 – 53; b) R. J. Silva, H. Nitsche, *Radiochim. Acta* **1995**, *70 – 71*, 377 – 396; c) S. G. Minasian, K. S. Boland, R. K. Feller, A. J. Gaunt, S. A. Kozimor, I. May, S. D. Reilly, B. L. Scott, D. K. Shuh, *Inorg. Chem.* **2012**, *51*, 5728 – 5736; d) K. P. Carter, R. G. Surbella III, M. Kalaj, C. L. Cahill, *Chem. Eur. J.* **2018**, *24*, 12747 – 12756.

[3] a) J. P. Kaszuba, W. H. Runde, *Environ. Sci. Technol.* **1999**, *33*, 4427 – 4433; b) M. R. Antonio, L. Soderholm, C. W. Williams, J. P. Blaudeau, B. E. Bursten, *Radiochim. Acta* **2001**, *89*, 17 – 25; c) S. Chatterjee, S. A. Bryan, A. J. Casella, J. M. Peterson, T. G. Levitskaia, *Inorg. Chem. Front.* **2017**, *4*, 581 – 594.

[4] a) E. Ansoborlo, O. Prat, P. Moisy, C. Den Auwer, P. Guilbaud, M. Carriere, B. Gouget, J. Duffield, D. Doizi, T. Vercouter, C. Moulin, V. Moulin, *Biochimie* **2006**, *88*, 1605 – 1618; b) R. J. Abergel, in *Metal Chelation in Medicine* (Eds.: R. Crichton, R. J. Ward, R. C. Hider), The Royal Society of Chemistry, Cambridge, UK, **2017**, pp. 183 – 212.

[5] a) D. M. Taylor, *Sci. Total Environ.* **1989**, *83*, 217 – 225; b) C. Vidaud, D. Bourgeois, D. Meyer, *Chem. Res. Toxicol.* **2012**, *25*, 1161 – 1175.

[6] R. J. Abergel, P. W. Durbin, B. Kullgren, S. N. Ebbe, J. Xu, P. Y. Chang, D. I. Bunin, E. A. Blakely, K. A. Bjornstad, C. J. Rosen, D. K. Shuh, K. N. Raymond, *Health Phys.* **2010**, *99*, 401 – 407.

[7] a) A. E. V. Gorden, J. Xu, K. N. Raymond, P. Durbin, *Chem. Rev.* **2003**, *103*, 4207 – 4282; b) A. Cilibrizzi, V. Abbate, Y.-L. Chen, Y. Ma, T. Zhou, R. C. Hider, *Chem. Rev.* **2018**, *118*, 7657 – 7701.

[8] a) P. W. Durbin, B. Kullgren, J. Xu, K. N. Raymond, P. G. Allen, J. J. Bucher, N. M. Edelstein, D. K. Shuh, *Health Phys.* **1998**, *75*, 34 – 50; b) B. Kullgren, E. E. Jarvis, D. D. An, R. J. Abergel, *Toxicol. Methods* **2013**, *23*, 18 – 26.

[9] a) M. Sturzbecher-Hoehne, G. J. P. Deblonde, R. J. Abergel, *Radiochim. Acta* **2013**, *101*, 359 – 366; b) G. J. P. Deblonde, M. Sturzbecher-Hoehne, R. J. Abergel, *Inorg. Chem.* **2013**, *52*, 8805 – 8811; c) M. Sturzbecher-Hoehne, B. Kullgren, E. E. Jarvis, D. D. An, R. J. Abergel, *Chem. Eur. J.* **2014**, *20*, 9962 – 9968; d) M. Sturzbecher-Hoehne, P. Yang, A. D'Aleo, R. J. Abergel, *Dalton Trans.* **2016**, *45*, 9912 – 9919.

[10] a) P. Zeh, J. I. Kim, C. M. Marquardt, R. Artinger, *Radiochim. Acta* **1999**, *87*, 23; b) G. A. Icopini, H. Boukhalfa, M. P. Neu, *Environ. Sci. Technol.* **2007**, *41*, 2764 – 2769; c) N. S. Shcherbina, I. V. Perminova, S. N. Kalmykov, A. N. Kovalenko, R. G. Haire, A. P. Novikov, *Environ. Sci. Technol.* **2007**, *41*, 7010 – 7015; d) Z. Zhang, B. F. Parker, T. D. Lohrey, S. J. Teat, J. Arnold, L. Rao, *Dalton Trans.* **2018**, *47*, 8134 – 8141.

[11] K. P. Carter, J. Jian, M. M. Pyrch, T. Z. Forbes, T. M. Eaton, R. J. Abergel, W. A. de Jong, J. K. Gibson, *Chem. Commun.* **2018**, *54*, 10698 – 10701.

[12] a) I. Captain, G. J. P. Deblonde, P. B. Rupert, D. D. An, M.-C. Illy, E. Rostan, C. Y. Ralston, R. K. Strong, R. J. Abergel, *Inorg. Chem.* **2016**, *55*, 11930 – 11936; b) A. Ricano, I. Captain, K. P. Carter, B. P. Nell, G. J. P. Deblonde, R. J. Abergel, *Chem. Sci.* **2019**, *10*, 6834 – 6843.

[13] K. T. Bennett, S. E. Bone, A. C. Akin, E. R. Birnbaum, A. V. Blake, M. Brugh, S. R. Daly, J. W. Engle, M. E. Fassbender, M. G. Ferrier, S. A. Kozimor, L. M. Lilley, C. A. Martinez, V. Mocko, F. M. Nortier, B. W. Stein, S. L. Thiemann, C. Vermeulen, *ACS Cent. Sci.* **2019**, *5*, 494 – 505.

[14] a) P. G. Allen, J. J. Bucher, D. K. Shuh, N. M. Edelstein, T. Reich, *Inorg. Chem.* **1997**, *36*, 4676 – 4683; b) M. A. Denecke, K. Dardenne, C. M. Marquardt, *Talanta* **2005**, *65*, 1008 – 1014; c) L. Soderholm, M. R. Antonio, C. Williams, S. R. Wasserman, *Anal. Chem.* **1999**, *71*, 4622 – 4628.

[15] M. P. Kelley, G. J. P. Deblonde, J. Su, C. H. Booth, R. J. Abergel, E. R. Batista, P. Yang, *Inorg. Chem.* **2018**, *57*, 5352 – 5363.

[16] a) M. D. Hawley, S. V. Tatawawadi, S. Piekarski, R. N. Adams, *J. Am. Chem. Soc.* **1967**, *89*, 447 – 450; b) D. G. Graham, S. M. Tiffany, W. R. Bell, W. F. Gutknecht, *Mol. Pharmacol.* **1978**, *14*, 644 – 653.

[17] a) T. Yamamura, N. Watanabe, T. Yano, Y. Shiokawa, *J. Electrochem. Soc.* **2005**, *152*, A830 – A836; b) L. S. Natrajan, A. N. Swinburne, M. B. Andrews, S. Randall, S. L. Heath, *Coord. Chem. Rev.* **2014**, *266 – 267*, 171 – 193; c) R. Gupta, J. V. Kamat, K. Aggarwal Suresh, *Radiochim. Acta* **2014**, *102*, 1069 – 1074.

[18] G. Skara, B. Pinter, P. Geerlings, F. De Proft, *Chem. Sci.* **2015**, *6*, 4109 – 4117.

[19] V. Mougel, J. Pécaut, M. Mazzanti, *Chem. Commun.* **2012**, *48*, 868 – 870.